ELSEVIER

Journal of Photochemistry and Photobiology A: Chemistry 115 (1998) 99–108

Journal of Photochemistry and Photobiology A:Chemistry

Electronic energy transfer in solution in naphthalene–anthracene, naphthalene–acridine and benzene–DANS bichromophoric compounds

Frank Schael [1], Mordecai B. Rubin, Shammai Speiser *

Department of Chemistry, Technion-Israel Institute of Technology, Technion City, Haifa 32000, Israel

Received 19 January 1998; received in revised form 4 March 1998; accepted 6 March 1998

Abstract

Intramolecular energy transfer (intraEET) in naphthalene–anthracene (**I**), naphthalene–acridine (**II**) and benzene–DANS (**III**) bichromophoric compounds was investigated by stationary absorption and fluorescence measurements in solution. Computer simulations of conformational distributions of compounds **I** (with $n = 1$, 3 and 6 methylene units as spacer groups) in the gas phase were performed and predict similar molecular structures for $n = 3$ and 6, which is consistent with previous observations in a supersonic jet expansion. In compounds **I**, fast intraEET (rate constant $k_{EET} > 1 \times 10^{10}\ s^{-1}$) was observed upon electronic excitation of the naphthalene moieties, whereas in compound **III** with 6 methylene units and an amide group as molecular spacer, a significantly slower intraEET was found ($k_{EET} = (1.0\ 0 \pm .5) \times 10^8\ s^{-1}$). The result is discussed within the framework of the Fermi Golden Rule expression. Differences in Franck–Condon weighted density of EET acceptor states and of the mutual orientation of the two chromophoric units were found to account for the different intraEET efficiencies. This work provides no evidence for intraEET in compounds **III**.

Keywords: Naphthalene–anthracene; Naphthalene–acridine; Benzene–DANS

---

1. Introduction

Photo-induced interactions between two chromophores incorporated in a single molecule have been of interest in photophysical research for the past three decades. These interactions are manifested in chemical reactions [1] intramolecular excimer and exciplex formation (intraEXF) [2], intramolecular electron transfer (intraELT) [3,4] and intramolecular electronic energy transfer (intraEET) [5]. Photoinduced IntraEET, intraELT and intraEXF between neutral chromophors are usually described by the following schemes:

$$D^*\text{–}B\text{–}A \xrightarrow{k_{EET}} D\text{–}B\text{–}A^* \tag{1}$$

$$D^*\text{–}B\text{–}A \xrightarrow{k_{ELT}} D^{\pm}\text{–}B\text{–}A^{\mp} \tag{2}$$

$$D^*\text{–}B\text{–}A \xrightarrow{k_{EXF}} [D\text{–}B\text{–}A]^* \leftrightarrow [D^{\pm}\text{–}B\text{–}A^{\mp}] \tag{3}$$

where D–B–A denotes a bichromophoric molecule consisting of the energy donor D, the molecular bridge B, and the energy acceptor A. The asterisk denotes the electronically excited states. The electronic absorption spectrum of a bichromophoric molecule can be described as a simple superposition of the absorption spectra of the two moieties D and A. The molecular bridge B serves as a molecular spacer without influencing the basic electronic structure of the two chromophores.

As both EET and ELT may be viewed as radiationless transitions between two electronic states, the rate constants k (k_{EET}, k_{ELT}) have some features in common [6–8] and should obey, in weakly coupled systems, where the transfer is nonadiabatic, the Fermi Golden Rule:

$$k=(2\pi/\hbar)V^2\mathrm{FCWDS} \tag{4}$$

where V is the electronic coupling matrix element and FCWDS is the Franck–Condon weighted density of states. Using an approach originally derived to describe ELT processes, FCWDS depends among other parameters on the free energy change ΔG, on the internal and solvent reorganization energy, λ_v and λ_s, and (in the single mode approximation) on the characteristic frequency $h\nu_v$ [9,10]. Because of the small charge migration in EET, λ_s is much smaller and the solvent dependence of k_{EET} is expected to be much smaller than that of k_{ELT}, in accordance with many experimental observations.

---

* Corresponding author.

[1] Institute für Physikalische und Theoretische Chemie, Universität Erlangen-Nürnberg, Egerlandstr. 3, D-91058 Erlangen, Germany.

1010-6030/98/$19.00 © 1998 Elsevier Science S.A. All rights reserved.
PII S1010-6030(98)00253-6

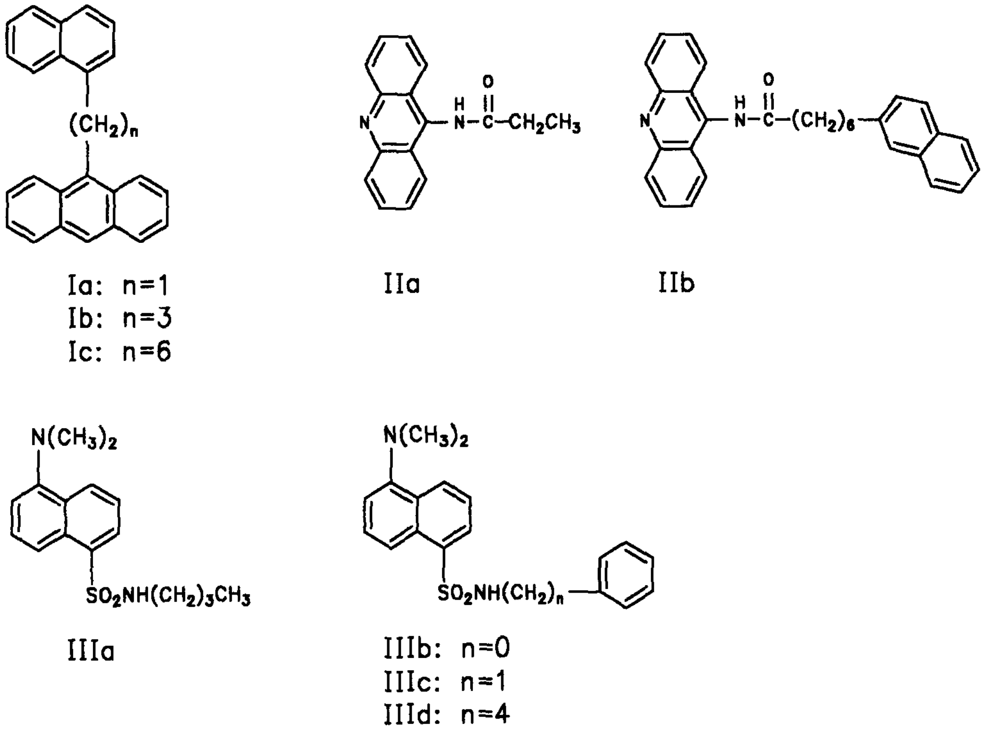

Ia: n=1
Ib: n=3
Ic: n=6

IIa

IIb

IIIa

IIIb: n=0
IIIc: n=1
IIId: n=4

Scheme 1. The bichromophoric compounds investigated in the present study.

The total electronic coupling matrix element for EET, $\mathbf{V}_{\text{EET}}$, can be partitioned into several contributions [11–13]:

$$\mathbf{V}_{\text{EET}}=V_{\text{Coul}}+V_{\text{short}}+V_{\text{rel}}+V_{\text{t-b}} \tag{5}$$

V_{Coul} denotes the direct coulombic contribution, which can be expressed in terms of dipole–dipole and higher multipole terms. It depends on the transition dipole moments of the involved transitions and on the mutual distance and the orientation of the transition dipole moments vectors. V_{short} accounts for the short-range contributions, which encompasses penetration and exchange interactions and depends crucially on the overlap between donor and acceptor orbitals. V_{rel} stands for coulombic contributions relayed by the connecting bridge and $V_{\text{t-b}}$ for through-bond mediated short-range contributions. V_{Coul} is generally assumed to be dominant at separation distances larger than 20 Å, whereas at shorter distances, in principle, all contributions have to be considered [12]. Because several contributions to EET can proceed simultaneously and competitively, model compounds in investigations of EET mechanisms are usually chosen so that one or more contributions to EET can be neglected. Where the dipole–dipole interaction is the dominant contribution to EET, the Förster formulation [14] can be obtained, whereas in cases where the exchange interaction is the most important contribution, the Dexter formulation [15] results from Eq. (4).

Valuable information can be obtained in comprehensive studies of bichromophoric molecules, in which more than one type of interchromophoric interactions are observed. For instance, IntraEXF in such systems indicates that conformations with close face-to-face orientations of the two chromophores exhibit high Boltzmann factors, which could provide valuable information for the interpretation of intraEET processes in the same molecule. In bichromophoric molecules, in which intraEET and intraELT proceed competitively, the comparison of k_{EET} and k_{ELT} within the framework of Eq. (4) can give insights into the parameters governing EET and ELT in the particular system [16].

The first investigations of singlet–singlet intraEET were reported by Weber [17,18], Weber and Teale [19] and by Schnepp and Levy [20]. Schnepp and Levy observed that in compounds **Ia** and **Ib** (see Scheme 1), where a naphthalenic moiety serves as energy donor D and an anthracene unit as the acceptor A, only anthracene fluorescence was emitted irrespective of the excitation wavelength. Weber and Teale reported for **IIIb** and **IIIc** (see Scheme 1) only fluorescence of the DANS (5-dimethylaminonaphthalene-1-sulfonamid) moiety after excitation of the benzene moiety.

From these and many other studies, it was generally concluded that systems exhibiting good spectral overlap and a flexible bridge structure are not suitable model compounds for the elucidation of short range EET mechanisms because (i) several contributions to EET may occur simultaneously and competitively, and (ii) the flexible structure complicates investigations of distance dependence of EET processes. Consequently, semi-rigid structures with chromophores involving forbidden transitions, in which the dipole–dipole contribution to EET was negligible, were developed [21–23]. The results showed good agreement with an exchange mechanism. Previously, rigid structures, in which the spatial orientation of the two chromophores excludes any significant contribution of direct dipole–dipole interaction, were designed to elucidate the mechanisms of through-bond, bridge mediated contributions to the transfer process [11].

Motivated by a number of reports, some of which are contradictory, about the photophysical processes in compounds **I** (vide infra), and our previous studies of this system in a supersonic jet expansion [24], the present study addresses the following aspects.

(i) Computer simulations of molecular conformations were carried out for compounds **I** in order to elucidate probability distributions of interchromophore distances and molecular structures.

(ii) IntraEET and intraEXF in **Ia** and **Ib** were reexamined, and **Ic** was synthesized to investigate the effect of a longer bridge on intraEET processes in this system.

(iii) The reference compound **IIa** and compound **IIb** (see Scheme 1), which exhibits a very similar donor moiety and a molecular bridge of similar length and flexibility as **Ic**, were synthesized to achieve a variation of the acceptor unit. The acridine-like acceptor moiety provides a different energy of the first excited singlet state and different redox properties as compared to the anthracence moiety in **Ic**. Energy gap effects on intraEET might be observable and intraEET and intraELT may act competitively in this compound.

(iv) The fluorescence and absorption properties of the benzene–DANS compounds **IIIb**, **IIIc** and **IIId** (See Scheme 1) were studied in polar and non-polar solvents. In extension of previous studies by Weber and Teale, we synthesized a reference compound **IIIa** and compound **IIId** to elucidate the effect of a longer bridge.

2. Experimental details

The compounds **Ia**, **Ib**, **Ic** [25], **IIa**, **IIb** (M.B. Rubin, unpublished results) and **IIIa**, **IIIb**, **IIIc**, **IIId** [26,27] were synthesized following literature procedures. The fluorescence spectra were measured with a Perkin Elmer LS 50 fluorescence spectrometer. Absorption spectra were detected with a Hewlett-Packard HP 8452A diode array spectrometer. The measurements were performed in 1 × 1 cm cuvettes. The solutions were deoxygenated by bubbling purified nitrogen through the solution and sealed off. The concentration of the fluorophores was chosen so that the optical density was not higher than 0.3 at the excitation wavelength to avoid internal filter effects. Fluorescence quantum yields (Φ_F) were determined against 9-methylanthracene and 1-methylnaphthalene in methylcyclohexane ($\Phi_F = 0.33$ and $\Phi_F = 0.21$, respectively [28]).

For the estimation of structures of the energetically most stable conformations, a set of conformations were computer-generated for each compound **Ia**, **Ib** and **Ic**, and subsequently the energy was minimized employing an AMBER force field method [29,30]. For the generation of the initial sets of conformations, $n+1$ rotational angles $\varphi_1, \varphi_2, \ldots, \varphi_{n+1}$ were used to describe a given conformation of each compound, where n is the number of methylene units in the molecular bridge. φ_1 and φ_{n+1} denote the angles for rotation around the C–C single bond attached to the anthracene and the naphthalene group, respectively, whereas $\varphi_2 \ldots, \varphi_n$ denote the angle for rotation around the single bonds within the chain. Three rotational isomers, trans, gauche$^+$, and gauche$^-$, were considered for $\varphi_2, \varphi, \ldots \varphi_n$. The angles ε_1 and φ_{n+1} rotate coincidentally with the angles of φ_2 and φ_n, respectively, taking the energy minima determined in a recent calculation for *n*-propylcarbazol and 2-propylnaphthalene [31]. The adopted values for the φ_1/φ_2 pairs were: 90°/0°, 100°/110°, 80°/ −110°, where 0° were taken at the *trans* conformation. The same values were employed for φ_{n+1}/φ_n and in addition −90°/0°, −100°/110°, −80°/−110° to account for the non-rotational symmetry of the 2-naphthyl group. For **Ia**, the quoted values for φ_1 and φ_{n+1} were combined. In this way, $2 \times 3^{n-1}$ conformations for **Ib** and **Ic** and 18 for **Ia** were generated and subsequently geometry-optimized. All computations were carried out on a personal computer (CPU 486/ 66 MHz).

3. Results and discussion

3.1. Naphthalene–anthracene bichromophoric compounds

3.1.1. Simulation of molecular conformations

The flexible polymethylene chains incorporated as molecular spacers in compounds **I** allow formation of a number of molecular conformations so that these compounds should be described by distributions of conformations. These distributions can be used to determine the parameters essential in evaluating through-space contributions to intraEET, such as mutual distances and orientations of the chromophoric units. The probability distribution of possible conformations is not known experimentally and is thus simulated. The primary objective of the computer simulation performed in this study is a comparison of the effect of the polymethylene chains in compounds **I** (i) on the gas phase structure of the energetically most stable conformations, and (ii) on the relative probability distribution of interchromophore distances. An ensemble of conformations were computer-generated for each compound **Ia**, **Ib** and **Ic** considering three rotational isomers for every C–C single bond within the chain and assuming plausible rotational angles. All structures were subsequently energy-minimized employing an AMBER force field method [30] (cf. Section 2). Thus, each molecular conformation obtained in this way corresponds to a minimum on the energy surface of the respective molecule. In order to save computing time, the relatively simple AMBER force field method was employed. Energy minimization of selected conformations with a method based on a MM2 force field gave similar results. Under the assumption that the distribution obeys the Boltzmann relation, the probability $p(i)$ of finding a certain conformation i in the respective ensemble is given by

$$p(i)=\exp(-E_i/kT)/\sum_i \exp(-E_i/kT) \qquad (6)$$

(E_i is the AMBER energy for the energy minimized conformation i.)

For each obtained conformation, the center-to-center distance r_{cc} between the two chromophoric units was calculated. The probability of finding a certain distance in the interval between $r_{cc}-\Delta r_{cc}$ and r_{cc} is the sum of the probabilities of all m conformations whose center-to-center distances fall within in this interval. The distribution is

$$p(r_{cc})=\sum_m p(m) \qquad \text{with } r_{cc}-\Delta\, r_{cc}\leq r_m\leq r_{cc} \qquad (7)$$

The r_{cc} distributions obtained with $T=293$ K and $\Delta r_{cc}=0.1$ Å are depicted in Fig. 1. The simulations result in relatively narrow distance distributions between ca. 3 and 5 Å despite the fact that the flexibility of the methylene chain allows distances up to 7.7 Å in **Ib** and 11.6 Å in **Ic**. While for **Ia** and **Ib** the r_{cc} distributions are narrow, and only few conformations exhibit significant Boltzmann factors, the distribution for **Ic** is broader and exhibits several maxima. The structures of the conformations with the highest Boltzmann factors are depicted as insets in Fig. 1. The r_{cc} of these conformations increases in the order **Ib** ($r_{cc}=3.3$ Å), **Ic** ($r_{cc}=3.8$ Å) and **Ia** ($r_{cc}=4.3$ Å). For **Ib** and **Ic**, the most stable conformations exhibit a sandwich-like orientation of the chromophoric units, while in **Ia** the single methylene group is not flexible enough to allow the two chromophores to attain close proximity.

The observation of association of the end groups in the force field simulation can be qualitatively understood if one considers the energy gain of ca. 7 kcal/mole, which results from attractive forces between the two chromophores [31]. This energy gain can be compared with the excess conformational energy of 0.5 kcal/mole for a *trans*-gauche, 1.4 kcal/mole for a gauche$^{\pm}$–gauche$^{\pm}$, and 3.1 kcal/mole for a gauche$^{\pm}$–gauche$^{\mp}$ conformation in *n*-pentane, where the energy was scaled so that the energy for the *trans–trans* conformation would be 0 [32]. The presented simulations are appropriate for conformation distributions of an isolated molecule in thermal equilibrium. In apparent consistency with the simulation results, the fluorescence excitation spectra of compounds **I** in an supersonic jet expansion show that the anthracene chromophores in **Ib** and **Ic** under these conditions are in very similar molecular environments, which are different from the environment of the anthracene chromophore in **Ia** [24,33].

In solution, however, solvation competes with the intramolecular association, the energy gain due to the attractive forces between the end-groups in folded conformations becomes less important, and broader r_{cc} distributions shifted to larger distances can be expected. Werner and Staerk simulated probability distributions of end-group distances in pyrene-$(CH_2)_n$-*N*,*N*-dimethylaniline compounds in solution and accounted for the weakening of the attractive forces by adjusting the parameters in the Lennard–Jones potential used to determine long-range energy terms [34]. The authors obtained for the compound with $n=6$, which has the same bridge as **Ic**, a r_{cc} distribution between ca. 5 and 15 Å with a maximum at ca. 13 Å and several minor maxima, which means that stretched conformations are predicted to play a more important role than folded ones. X-ray structure analysis of **Ib** and **Ic** further support this view. Stretched structures with $r_{cc}=7.0$ and 11.3 Å were observed in the crystal phase of **Ib** and **Ic**, respectively [35] (F. Schael, M. Kapon, M.B. Rubin, S. Speiser, unpublished results).

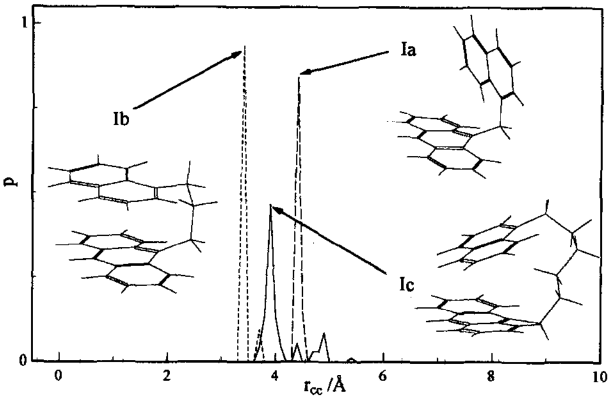

Fig. 1. Center-to-center distance (r_{cc}) distributions for **Ia**, **Ib** and **Ic** in the gas phase. The insets show calculated structures of the energetically most stable conformations. The simulations were performed with an AMBER force field method.

NMR and single photon counting investigations of diastereomeres of 2,4-di(2-pyrenyl)pentane by Reynders et al. showed (i) the presence of a number of conformations, where the conformation with sandwich-like orientation of the end groups was not the dominant one or even not detected at all in toluene-d_8 and chloroform-d between −49° and 60°C, and (ii) that rapid interconversion on a subnanosecond timescale takes place after photoexcitation of the pyrene moiety in toluene at 25°C [36]. It appears that not only the conformational distributions in the electronic ground states are important, but in addition, dynamic processes in the electronically excited states have to be considered in solution.

3.1.2. Fluorescence and intraEET studies

Fig. 2 shows the absorption and fluorescence spectra of compounds **I** in methylcyclohexane. The spectra were measured with deoxygenated solutions. The absorption spectra of **Ia**, **Ib** and **Ic**, which are in agreement with the spectra reported by Rona and Feldman [26] for **Ia** and **Ib**, can be described as simple superpositions of the absorption spectra of 9-methylanthracene (**9-MA**) and of 1-methylnaphthalene (**1-MN**). The fluorescence emission spectra of compounds **I** are similar to the spectrum of **9-MA**, except that the relative intensities of the fluorescence bands are different. The difference in the relative intensities of the fluorescence bands is most pro-

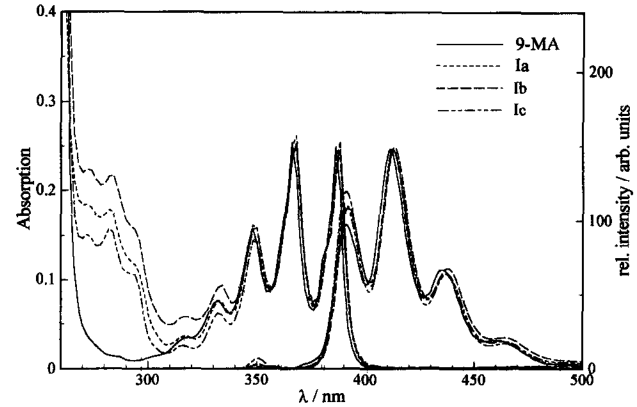

Fig. 2. Absorption and fluorescence spectra of **Ia**, **Ib** and **Ic** and of 9-methylanthracene (**9-MA**) in methylcyclohexane at room temperature. The maxima of the fluorescence spectra were normalized to the long-wavelength absorption maxima.

nounced at the 0–0 fluorescence bands, probably due to different electronic ground state geometries, which result in different Franck–Condon factors for the observed transitions. In Fig. 3, the fluorescence emission spectra of **Ia**, **Ib** and **Ic** normalized at the 0–0 fluorescence band are displayed. The fluorescence spectrum of **Ib** is red-shifted by about 1 nm and exhibits at long wavelengths slightly higher intensity than the spectra of the other compounds. The higher long-wavelength intensity can be simply due to different electronic ground-state geometries of the compounds or to an exciplex emission, which is more pronounced in the spectrum of **Ib** than in the spectra of **Ia** and **Ic**. But the difference spectrum between the spectrum of **Ib** and the spectrum of **9-MA** is not structureless, and the same holds true for the difference between the **Ib** spectrum and the **Ia** spectrum. This seems to be in contradiction to any hypothesis that an exciplex emission contributes to the spectral shape of the **Ib** fluorescence spectrum. On the other hand, the possible distortion of the ground state geometries of **Ia** and **Ic** due to the substitution and its influence on the shape of the fluorescence spectra, puts doubt on the suitability of **Ia** and **9-MA** as reference compounds for this purpose. However, Desvergne et al. [37] observed a weak, structureless difference spectrum between the fluorescence spectrum of **Ib** and the spectrum of 9-hexylanthracene in methylcyclohexane at room temperature, and interpreted this as emission of an intramolecular exciplex. Exciplex emission was also recorded by Ferguson et al. [38] at 293 K in a microcrystal and by Chandros in a matrix at 77 K after partial photocleavage of an photocyclomer of **Ib** [39].

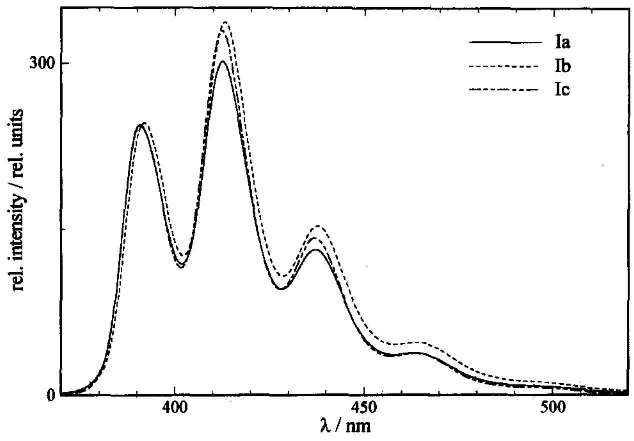

Fig. 3. Fluorescence emission spectra of **Ia**, **Ib** and **Ic** in methylcyclohexane at room temperature. The spectra were normalized at 405 nm.

Under the conditions employed by Ferguson et al. and Chandros et al., **Ib** is chemically formed in a sandwich-like orientation of the two chromophores. The latter studies reveal that an intramolecular exciplex can be formed in **Ib**, whenever a suitable sandwich-like orientation of the chromophores is achieved. From excimer formation studies in solution, it is known that excimer formation between aromatic chromophores linked by polymethylene chains occurs almost exclusively with $n = 3$ [40,41]. Since similar mutual orientations of the chromophores in excimers and exciplexes can be expected, it is more likely to observe exciplex emission in **Ib** than in any other compound of this series. However, from the absence of any pronounced exciplex emission, it can be concluded that under these conditions, intraEXF plays a minor role in compounds **I** following the excitation of the anthracene moiety. The fluorescence emission spectra of compounds **I** at room temperature and at 77 K are independent of the excitation wavelength and correspond to exclusively anthracene-like emission. Under the assumption that the absence of naphthalenic emission is due to an intramolecular quenching process, the rate constant of fluorescence quenching of the naphthalene moiety can be estimated with Eq. (8):

$$\Phi_F^0/\Phi_F^{280} = 1 + k_q \tau_F^0 \qquad (8)$$

where $\Phi_F{}^0$ and $\tau_F{}^0$ denote the fluorescence quantum yield and lifetime of the naphthalene moiety in the absence of any interchromophoric interaction and $\Phi_F{}^{280}$ the fluorescence quantum yield of the naphthalene moiety in the bichromophoric molecule. With the data for **1-MN** taken for $\Phi_F{}^0$ and $\tau_F{}^0$ (i.e., $\Phi_F{}^0 = 0.21$ and $\tau_F{}^0 = 67$ ns [28]), and an estimated upper limit for $\Phi_F{}^{280} < 0.0003$, Eq. (8) yield $k_q > 1 \times 10^{-10}$ s^{-1}. The absence of any naphthalenic emission upon excitation of the naphthalene moiety in compounds **I** is in line with earlier reports by Schnepp and Levy [20], but in case of **Ib** in contrast to reports by Desvergne et al. [37] and Ferguson et al. [38] who observed very weak naphthalenic emission in **Ib** in methylcyclohexane at room temperature and at 77 K, respectively.

The fluorescence quantum yields determined in this work are summarized in Table 1. The results obtained here for **Ia** and **Ib** are in agreement with the results reported by Schnepp and Levy (cf. Table 1). It is notable that **Ic** exhibits very similar fluorescence properties as **Ib**. The fluorescence quantum yields upon excitation of the anthracene moiety of **Ib** and **Ic** ($\Phi_F = 0.52 \pm 0.06$ and $\Phi_F = 0.54 \pm 0.06$, respectively) are slightly higher than the fluorescence quantum yields of **Ia** and **9-MA** ($\Phi_F = 0.38 \pm 0.06$ and $\Phi_F = 0.33$ [28], respectively). The occurrence of singlet–singlet intraEET from the naphthalene to the anthracene moiety in compounds **I** is

Table 1
Fluorescence quantum yields of **Ia**, **Ib** and **Ic** upon excitation of the anthracene unit at 340 nm (Φ_F^{40}) and upon excitation of the naphthalene group at 280 nm (Φ_F^{280}) and EET efficiencies (Φ_{EET}) at room temperature

	Φ_F^{340}	Φ_F^{280}	Φ_{EET}
Ia	0.38 ± 0.06 (0.39 ± 0.03)	0.33 ± 0.06 (0.41 ± 0.07)	0.87 ± 0.21 (0.95 ± 0.20)
Ib	0.54 ± 0.06 (0.49 ± 0.03)	0.51 ± 0.06 (0.51)	0.94 ± 0.15 (0.96)
Ic	0.52 ± 0.06	0.48 ± 0.06	0.92 ± 0.16

The values given in brackets are derived from the results reported by Schnepp and Levy [20] assuming $\Phi_F = 0.33$ for **9-MA** and $\Phi_F^{280} = 0.51$ for **Ic**.

proved by the fact that the fluorescence excitation spectra (not shown) monitored at the anthracene emission wavelengths resemble the absorption spectra, and by the absence of any naphthalene-like emission upon excitation in the wavelength region around 280 nm, where most of the absorption stems from the naphthalene moiety. The EET efficiencies Φ_{EET} determined for compound **I** are unity within experimental uncertainty. For **Ia**, a lower value of $\Phi_{EET} = 0.8$ was reported by Farkas et al. without statement of experimental error [42]. Because of this high observed intraEET efficiency, other non-radiative deactivation processes of the excited naphthalene moiety appear to be less important, and the rate constant of quenching of the naphthalenic fluorescence provides a basis for estimation of the rate constant of intraEET. Thus, singlet–singlet intraEET in compounds **I** occurs with a rate constant of $k_{EET} > 1 \times 10^{10}\ s^{-1}$. No significant temperature effect on singlet–singlet EET was observed as indicated by the absence of naphthalenic emission at room temperature and at 77 K. The observation of generally very high Φ_{EET} in compounds **I**, which was reported previously for $n = 1$, 2 and 3, appears to persist to at least $n = 6$.

From the simulations and considerations in Section 3.1, it follows that **Ib** and **Ic** in the electronic ground state are likely to form conformational distributions in solution, in which stretched rather than folded conformations exhibit large Boltzmann factors. If no conformational changes occur after photoexcitation, all contributions to the electronic coupling matrix element V_{EET} can be expected to vary in the series **Ia**, **Ib**, **Ic**. V_{Coul} and V_{short} vary due to variations of the mutual distances and orientations of the end groups and V_{rel} and $V_{t\text{-}b}$ vary because of the variation of the bridge length. In general, a decrease of V_{EET} in the order **Ia**, **Ib**, **Ic** can be expected, whereas FCWDS is constant. It may therefore be concluded that k_{EET} for compound **I** are very high, probably due to high FCWDS, so that the variations achieved in V_{EET} are not sufficient to let resulting variations in k_{EET} become observable in the stationary measurements performed in this study.

3.2. Naphthalene–acridine bichromophoric compound

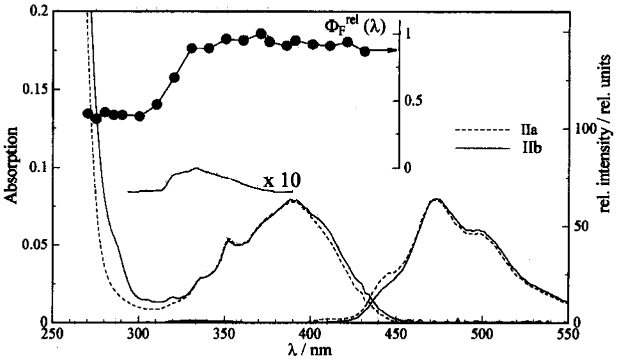

Fig. 4. Absorption and fluorescence spectra (upon excitation at 285 nm) of **IIa** and **IIb** in methanol/0.01 N NaOH at room temperature. The short-wavelength emission of **IIb** is multiplied by 10 and vertically displaced for clarity. In the inset, the relative fluorescence quantum yield Φ_F^{rel} (see text for definition) is plotted vs. the excitation wavelength.

Fig. 4 shows the absorption and fluorescence spectrum of **IIa** and **IIb** in deoxygenated methanol/0.01 N NaOH. The spectra of both compounds are very similar, except that the absorption spectrum of **IIb** exhibits a shoulder at around 290 nm, and in the fluorescence spectrum of **IIb** upon excitation at 280 nm, an additional emission between 310 and 360 nm is discernible. Both features can be identified as being due to absorption and emission from the naphthalene moiety in **IIb**. The acridine chromophore has a considerable extinction coefficient at the wavelength of naphthalene absorption. Attempts to detect fluorescence of the acridine moiety in hydrocarbon solvents were not successful, presumably due to combination of low solubility and low fluorescence quantum yields. Thus, investigations were carried out with methanol and methanol/0.01 N NaOH solutions. The absorption spectra of **IIa** and **IIb** are considerably different from the absorption spectrum of the parent chromophore 9-aminoacridine (**9-AA**) in alkaline water, which exhibits a vibrational structure with a shoulder at the long-wavelength edge at ca. 430 nm [43,44], whereas the fluorescence emission spectra are very similar to the spectrum of **9-AA** with only slightly different relative intensities of the vibrational bands. The fluorescence excitation spectra of **IIa** and **IIb** monitored between 430 and 550 nm correspond to the absorption spectra, while spectra monitored between 400 and 420 nm reveal the minor presence of a second fluorescent species. The excitation spectra monitored between 400 and 420 nm are independent of the presence of NaOH, while this is not the case for spectra monitored between 430 and 550 nm. In methanol/0.01 N NaOH solution, the fluorescence emission spectra and quantum yields of **IIa** and **IIb** are almost identical and independent of the excitation wavelength between 420 and 330 nm. It should be noted that the excited state properties of acridine and its derivatives were found to depend strongly on solvent, temperature and substitutions. Experimental observations were interpreted in terms of changes in nature, ordering and mixing of the two lowest excited singlet states [43,45]. Recently, tautomeric phenomena in **9-AA** were investigated and the observations described above appear to be consistent with such processes, which are probably more complex in **IIa** and **IIb** due to the presence of the amide group [44,46]. Further-more, hydrogen abstraction after photoexcitation in hydrogen donating solvents [47] and protonation equilibria [48,49] were observed. It was not the purpose of the present study to establish the origin of the observed solvent dependence of the fluorescence and absorption properties of **IIa** and **IIb**, which deserves a study on its own. However, we conclude that under our conditions **IIa** is a suitable reference compound for **IIb**.

The fluorescence quantum yields of both compounds excited between 430 and 330 nm are the same within experimental uncertainty ($\Phi_F = 0.24 \pm 0.04$ for **IIa** and $\Phi_F = 0.22 \pm 0.04$ for **IIb**), while the fluorescence quantum yield of the naphthalenic emission upon excitation of **IIb** at 280 nm is $\Phi_F^{280} = 0.006 \pm 0.002$. According to Eq. (8), the rate constant of fluorescence quenching of the naphthalene moiety is therefore $k_q = (6 \pm 2) \times 10^8$ s^{-1}, where $\Phi_F^0 = 0.21$ and $\tau_F^0 = 59$ ns of 2-methylnaphthalene [28] was assumed. The relative fluorescence quantum yield Φ_F^{rel}, defined as the ratio between the acridine-like fluorescence quantum yields of **IIb** and of **IIa**, exhibits a remarkable dependence on the excitation wavelength: Φ_F^{rel} decreases from 0.93 ± 0.07 in the 430–330 nm region to 0.39 ± 0.02 in the 300–270 nm region, where the naphthalene chromophore absorbs (cf. Fig. 4). Occurrence of singlet-singlet intraEET from the naphthalene to the acridine chromophore in **IIb** is established by the fluorescence excitation spectra monitored at 475 nm, which resembles the absorption spectrum. The excitation wavelength dependence of Φ_F^{rel} and the observation of residual naphthalenic emission is consistent with inefficient intraEET. After correction for direct absorption of the acridine-like chromophore in the short wavelength region, the EET efficiency $\Phi_{EET} = 0.17 \pm 0.02$ was obtained. k_{EET} can then be calculated with Eq. (9),

$$k_{EET} = \Phi_{EET}(1/\tau_F^0 + k_q) \tag{9}$$

from which $k_{EET} = (1.0 \pm 0.5) \times 10^8$ s^{-1} is obtained. Thus, k_{EET} for **IIb** is at least two orders of magnitude smaller than k_{EET} for **Ic** ($k_{EET} > 1.0 \times 10^{10}$ s^{-1}), which exhibits a very similar donor moiety (1-naphthyl in **Ic**, 2-naphthyl in **IIb**) and a similar molecular bridge (6 methylene units in **Ic**, 6 methylene units and an amide group in **IIb**).

k_{EET} may be discussed in the framework of Eqs. (4) and (5). V_{short} can be expected to play a minor role due to the relative large interchromophore distances expected for **IIb** and **Ic** in solution. V_{rel} and $V_{t\text{-}b}$ are probably similar in both compounds, if not smaller in **IIb** than in **Ic** because of the longer bridge. V_{Coul} depends on the transition dipole moments of the involved electronic transitions and on the probability distributions of mutual distances and orientations of the transition dipole moment vectors [11]. From molecular mechanics calculations, $r_{cc} = 12.7$ Å and 11.6 Å, respectively, were obtained for **IIb** and **Ic** in all-*trans* conformation. Due to the similar flexibility and length of the molecular bridges, the probability distributions of mutual distances in solution may therefore assumed to be similar in **IIb** and **Ic**, whereas appropriate simulations are needed to describe distributions of the orientation factors. Examining the spectral overlap between the (normalized) donor fluorescence and the acceptor absorption (in l mol^{-1} cm^{-1}) spectra of both compounds, one finds $J_{d\text{-}d} = 3.8 \times 10^{-15}$ and 1.6×10^{-15} cm^6 mol^{-1} for **Ic** and **IIb**, respectively. The obtained values for $J_{d\text{-}d}$, which contain information about the transition dipole moments and FCWDS, indicate that dipole–dipole interaction is a major contribution to intraEET in both compounds. If the observed intraEET is purely due to dipole–dipole interaction, k_{EET} is proportional to $J_{d\text{-}d}$ [14]. Thus, the observed $J_{d\text{-}d}$ of **Ic** and **IIb** can account only for a ca. twofold increase of k_{EET} in **Ic** compared to k_{EET} in **IIb** and not only FCWDS but also V_{EET} appear to be different in both compounds. In V_{EET}, the most likely parameter, which is different for both compounds, is the mutual orientation of the two chromophoric units. Anthracene has a second transition below the naphthalene ^1L_b state [50] and so does **9-AA** [51], which, lacking a better model, might be taken as a model for the acceptor states in **IIb**. In both anthracene and **9-AA**, the lowest excited singlet state is long-axis polarized, while the second is short-axis polarized with respect to the aromatic plane. Thus, only the chemical difference of the bridge and the different substitution position of the naphthalene moiety is likely to contribute to possible different mutual orientations of the two chromophoric units in **Ic** and **IIb**.

Interestingly, the different intraEET behaviour of **Ic** and **IIb** is even more pronounced in a supersonic jet expansion. Under these conditions, very high intraEET efficiency upon excitation of the naphthalene moiety was observed for **Ic** [33], whereas no indication for intraEET at all was found in **IIb** [52].

The observation that k_q is significantly higher than k_{EET} implies that the electronically excited naphthalene moiety in **IIb** decays non-radiatively to the ground electronic state through a channel unavailable to the separate chromophore. The rate constant for the acceptor-induced non-radiative decay process is $k_{nr} = k_q - k_{EET} = (5 \pm 2) \times 10^8$ s^{-1}. A possible nonradiative decay channel to be considered is intraELT. Estimation of the standard free energy change for intraELT (ΔG_{ELT}) from the electronically excited naphthalene to the acridine moiety according to the Weller equation without work term yields $\Delta G_{ELT} = -1.20$ eV in acetonitrile solution. In the estimation, the halfwave reduction potential $E_{red}^{1/2} = -1.25$ V of **9-AA** [53], the halfwave oxidation potential $E_{ox}^{1/2} = 1.45$ V [53] and $E(S_1) = 3.90$ eV [28] of **2-MN** were employed (the quoted potentials were measured in polar solvents vs. SCE). Although the estimated value for ΔG_{ELT} might be subject to considerable error due to the uncertainties in the redox potential, it follows, however, that ΔG_{ELT} is most probably exergonic, and thus intraELT is very likely to contribute to the non-radiative decay of the electronically excited naphthalene moiety in **IIb**.

3.3. Benzene–DANS bichromophoric compounds

Fig. 5 shows the absorption and fluorescence spectra of compounds **III** in methylcyclohexane and methanol. The

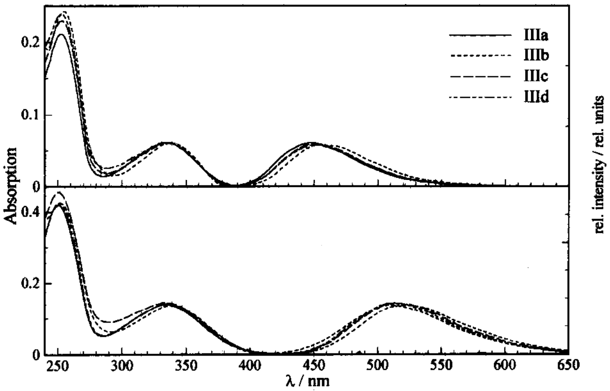

Fig. 5. Absorption and fluorescence spectra of **IIIa**, **IIIb**, **IIIc** and **IIId** in air-saturated methylcyclohexane (upper part) and methanol (lower part). The fluorescence spectra were normalized to the maxima of the long-wavelength absorption maxima.

spectra were recorded with air-saturated solutions. Fluorescence quenching effects due to oxygen can have only a minor effect on the fluorescence properties because of the relatively short fluorescence lifetime of the DANS chromophore in solution (for example, $\tau_F = 8.1$ ns in *n*-hexane [54]). The two apparent absorption bands of **IIIa** exhibit a 5-nm red shift compared to the absorption bands of compounds **IIIa**, **IIIc** and **IIId**. The maximum of the emission spectrum of **IIIb** is shifted by 8 ± 2 nm with respect to the maxima of the emission spectra of **IIIa**, **IIIc**, and **IIId**. A similar shift of 10 nm between the maxima of the emission spectra of **IIIb** and **IIIc** in ethanol was reported previously [19]. Thus, the electronic structure of the DANS chromophore in **IIIb** is influenced by the substitution to a somewhat higher degree than **IIa**, **IIIc** and **IIId**. The emission spectra exhibit a large spectral shift to the red with increasing solvent polarity, whereas the solvent shift of the absorption spectra is not dramatic. This behaviour is characteristic for the DANS chromophore and was established as being due to a solvent relaxation phenomenon in combination with a change in the nature of the emitting state ([55,56] and references therein). For the parent chromophore 1-aminonaphthalene, it was shown that the appropriate label for the emitting state is ^1L_b and ^1L_a/CT in polarand non-polar solvents, respectively [56].

It is clear from the spectra in Fig. 5 that a distinct absorption band due to the absorption of the benzene moiety in **IIIb**, **IIIc** and **IIId** is discernible neither in polar nor in non-polar solvents. In the spectral region where the benzene chromophore is expected to absorb (240–260 nm) the DANS chromophore exhibits a strong absorption band. This band can be assigned as a transition into a $^1A_g^-$ state [57]. The extinction coefficient (ϵ_s) of the reference compound **IIIa** at 260 nm was determined as 25,000 ± 2500 l mol^{-1} cm^{-1} in methylcyclohexane. This value may be compared to $\varepsilon_s = 225$ l mol^{-1} cm^{-1} at 254 nm for toluene and to $\varepsilon_s = 970$ l mol^{-1} cm^{-1} at 273 nm for aniline in cyclohexane solution [58]. The difference between the absorption spectra of **IIIb–IIId** and of **IIIa** reveal that the benzene-like absorption at 255 nm contributes not more than 10% to the total absorption at this wavelength. It is, thus, not surprising that the absorption of the benzene moiety is not discernible in the absorption spectra of **IIIb–IIId**, complicating distinct excitation of the benzene moiety and observation of subsequent intraEET.

The relative fluorescence quantum yield upon excitation at 340 nm, $\Phi_F^{rel,340}$, in methylcyclohexane solution for all four compounds is the same within experimental uncertainty (cf. Table 2). This means that the benzene-like substitution does not change the deactivation of the first excited singlet state of the DANS chromophore to a significant degree. No benzene-like emission was observable upon excitation at 260 or shorter wavelength, where the benzene moiety is expected to absorb. Φ_F^{rel} of **IIIa** and **IIIc** did not depend on the excitation wavelength within experimental uncertainty. **IIIc** and **IIId** exhibit fluorescence properties very similar to the reference compound **IIIa**. For **IIIb** a decrease of Φ_F^{rel} to approximately 0.4 in methylcyclohexane upon excitation at 240 nm was observed. This behaviour is also reflected in the fluorescence excitation spectra (not shown). Our result is consistent with the decrease of Φ_F of ca. 30% in **IIIb** in comparison to **IIIc** upon excitation at 260 nm in ethanol reported by Weber and Teale [19]. This observation was interpreted in that work as the effect of intraEET being more efficient in **IIIc** as in **IIIb**. However, given the fact that the absorption at the excitation wavelength is almost exclusively due to absorption of the DANS moiety, it seems unlikely that non-radiative deactivation processes of the benzene moiety are responsible for the observed decrease in Φ_F^{rel} in **IIIb**. The observed decrease of Φ_F^{rel} in **IIIb** might be rather viewed as being due to the introduction of a non-radiative decay channel for the $^1A_g^-$ DANS state by the substitution in **IIIb**, which is not accessible in the other compounds **IIIa**, **IIIc** and **IIId**.

We conclude from the results described above that compound **III** do not represent a suitable bichromophoric system for investigations of intraEET upon excitation of the benzene-like chromophore. If anything, only the absence of benzene-like emission in **IIIb**, **IIIc** and **IIId** might be taken as a hint for the occurrence of interchromophoric interactions between the electronically excited benzene chromophore and the DANS moiety, but the absence of any distinct benzene-like absorption in the spectra of **IIIb**, **IIIc** and **IIId** prevents any further conclusions. We suspect that in the work of Weber and Teale, the comparison of **IIIb** with **IIIc** instead of com-

Table 2
Relative fluorescence quantum yields Φ_F^{rel} (at the excitation wavelengths given in the superscripts) of **IIIa**, **IIIb**, **IIIc** and **IIId** and wavelength of maximum absorption λ_{max}^{abs} and fluorescence λ_{max}^{flu} in air-saturated methylcyclohexane solution at room temperature

	$\Phi_F^{rel,340}$ (± 0.1)	$\Phi_F^{rel,240}$ (± 0.1)	λ_{max}^{abs}/nm (± 2 nm)	λ_{max}^{flu}/nm (± 2 nm)
IIIa	1.0	1.0	334	446
IIIb	1.0	0.4	340	456
IIIc	0.9	0.9	335	448
IIId	1.0	0.7	334	450

parison to a suitable reference compound lead to the misinterpretation, that intraEET is responsible for the observed less intensive DANS fluorescence in **IIIb** than in **IIIc** upon excitation in the $^1A_g^-$ absorption band.

4. Summary

The flexible polymethylene chains incorporated as molecular bridges in the bichromophoric compounds investigated in the present study allow formation of a number of molecular conformations, so that these compounds in solution should be described by distributions of conformations. Since the conformational distributions are not known experimentally, computer simulations were carried out on the basis of simple molecular mechanics calculations. Probability distributions of center-to-center distances for the naphthalene anthracene compounds **I** were obtained, in which the interchromophoric distances between the two chromophoric units fall in a relatively narrow region between ca. 3 and 5 Å for **Ia**, **Ib** and **Ic**, despite the fact that the spacer group in **Ib** and **Ic** allows for much longer distances in stretched conformations. For **Ib** and **Ic**, structures for the energetically most stable conformations were obtained with sandwich-like orientation of the chromophoric units. Whereas these simulations provide an appropriate description of isolated molecules in thermal equilibrium, in solution, solvation competes with intramolecular association, and stretched rather than folded conformations can be expected to exhibit high Boltzmann factors [59,60].

Compound **I** exhibit fast intramolecular electronic energy transfer (intraEET) upon excitation of naphthalene moiety. For the rate constant of intraEET, k_{EET}, a lower limit of $1 \times 10^{10}\ \mathrm{s}^{-1}$ was obtained. Thus, the intraEET process, which was observed previously by Schnepp and Levy in **Ia** and **Ib**, happens to be very fast even in **Ic**, which has a molecular bridge of 6 methylene units. Since the electronic coupling matrix element $\mathbf{V}_{\mathrm{EET}}$ is expected to change in the series of compounds **I**, due to the variation of the bridge length and because of different distance distributions in solution, the Franck–Condon weighted density of EET acceptor states in this system is presumably very high and does not allow any changes in $\mathbf{V}_{\mathrm{EET}}$ to be discernible in the rate constants k_{EET} determined in this study.

In the naphthalene acridine bichromophoric compound **IIb**, intraEET (with $k_{\mathrm{EET}} = (1.0 \pm 0.5) \times 10^8\ \mathrm{s}^{-1}$) and an acceptor-induced non-radiative decay process of the naphthalene moiety (rate constant $k_{\mathrm{nr}} = (5 \pm 3) \times 10^8\ \mathrm{s}^{-1}$) was observed. The free energy change for intraELT from the excited naphthalene to the acridine moiety $\Delta G_{\mathrm{ELT}} = -1.20$ eV was estimated from halfwave redox potentials of the parent chromophores. It is, therefore, very likely that intraELT contributes to the observed non-radiative decay of the naphthalene moiety in **IIb**. The decrease in k_{EET} by at least two orders of magnitude in **IIIb** compared to k_{EET} in **Ic**, which has a very similar donor moiety and a molecular spacer group of similar length and flexibility, is probably due to different Franck–Condon weighted density of acceptor states and due to different distributions of mutual orientations of the two chromophoric units. The latter effect is caused by the change in substitution in the naphthalene donor (1-naphthyl in **Ic**, 2-naphthyl in **IIb**) and by the fact that the molecular bridges (6 methylene units in **Ic**, 6 methylene units and an amide group in **Iib**) are not completely identical. Further systematic studies with various acceptor units are needed in order to separate both effects. Work in this laboratory is now in progress to obtain realistic probability distributions of mutual distances and orientations of the chromophoric units in solution.

In the benzene–DANS bichromophoric compounds **III**, the high spectral overlap between the absorption spectra of the donor and the acceptor units prevents any reliable evaluation of intraEET in these compounds. This is in contrast to earlier interpretations of fluorescence properties of **IIIb** and **IIIc**, no evidence for occurrence of intraEET in compounds **III** was found.

Acknowledgements

Financial support by the US-Israel Binational Science Foundation is gratefully acknowledged. F.S. thanks the Max-Planck-Gesellschaft for a MINERVA postdoctoral fellowship.

References

[1] H.D. Becker, Chem. Rev. 93 (1993) 145.
[2] F.C. DeSchryver, N. Boens, T. Put, Adv. Photochem. 10 (1977) 359.
[3] M.A. Fox, M. Chanon (Eds.), Photoinduced Electron Transfer, Parts A–D, Elsevier, Amsterdam, 1988.
[4] G.J. Karvanos, Fundamentals of Photoinduced Electron Transfer, VCH Publishers, New York 1993.
[5] S. Speiser, Chem. Rev. 96 (1996) 1953.
[6] J.F. Endicott, Acc. Chem. Res. 21 (1988) 59.
[7] M.E. Sigman, G.L. Closs, J. Phys. Chem. 95 (1991) 5012.
[8] S.H. Lin, W.Z. Xiao, W. Dietz, Phys. Rev. E 47 (1993) 3698.
[9] R.A. Marcus, Annu. Rev. Phys. Chem. 15 (1964) 155.
[10] J. Ulstrup, J. Jortner, J. Chem. Phys. 63 (1975) 4358.
[11] G.D. Scholes, K.P. Ghiggino, A.M. Oliver, M.N. Paddon-Row, J. Phys. Chem. 97 (1993) 11871.
[12] G.D. Scholes, K.P. Ghiggino, J. Phys. Chem. 98 (1994) 4580.
[13] G.D. Scholes, K.P. Ghiggino, J. Photochem. Photobiol. A: Chem. 80 (1994) 355.
[14] T. Foerster, Z. Electrochem. Angew. Phys. Chem. 53 (1949) 93.
[15] D.L. Dexter, J. Chem. Phys. 21 (1953) 836.
[16] G.L. Closs, P. Piotrowiak, J.M. MacInnis, G.R. Fleming, J. Am. Chem. Soc. 110 (1988) 2652.
[17] G. Weber, Trans. Faraday Soc. 44 (1950) 185.
[18] G. Weber, Nature (London) 180 (1957) 1409.
[19] G. Weber, F.W.J. Teale, Trans. Faraday Soc. 54 (1958) 640.
[20] O. Schnepp, M. Levy, J. Am. Chem. Soc. 84 (1962) 172.
[21] S. Hassoon, H. Lustig, M.B. Rubin, S. Speiser, J. Phys. Chem. 88 (1984) 6367.
[22] S. Speiser, S. Hassoon, M.B. Rubin, J. Phys. Chem. 90 (1986) 5085.
[23] S.-T. Levy, M.B. Rubin, S. Speiser, J. Am. Chem. Soc. 114 (1992) 10747.

[24] G. Rosenblum, D. Grosswasser, F. Schael, M.B. Rubin, S. Speiser, Chem. Phys. Lett. 263 (1996) 441.
[25] P. Rona, U. Feldman, J. Chem. Soc., 1958, 1737.
[26] G. Weber, Biochem. J. 51 (1952) 155.
[27] A. Okomoto, K. Uchiyama, I. Mita, Bull. Chem. Soc. Jpn. 55 (1982) 3068.
[28] S.L. Murov (Ed.), Handbook of Photochemistry, Marcel Dekker, New York, 1973.
[29] S.J. Weiner, P.A. Kollmann, D.A. Case, U.Ch. Singh, C. Ghio, G. Alagona, S. Profeta, P. Weiner, J. Am. Chem. Soc. 106 (1984) 765.
[30] Program Hyperchem 3, Hypercupe, 1993.
[31] G. Rosenblum, S. Speiser, J. Chem. Phys. 102 (1995) 9149.
[32] M. Lal, D. Spencer, Mol. Phys. 22 (1971) 649–659.
[33] G. Rosenblum, PhD Thesis, Technion, Haifa, Israel, 1997.
[34] U. Werner, H. Staerk, J. Phys. Chem. 97 (1993) 9274.
[35] Y. Mori, K. Maeda, J. Chem. Soc., Perkin Trans. 2 (1995) 113.
[36] P. Reynders, H. Dreeskamp, W. Kuehnle, K.A. Zachariasse, J. Phys. Chem. 91 (1987) 3982.
[37] J.-P. Desvergne, N. Bitit, A. Castellan, H. Bouas-Laurent, J. Chem. Soc., Perkin Trans. II (1983) 109.
[38] J. Ferguson, A.W.-H. Mau, P.O. Whimp, J. Am. Chem. Soc. 101 (1979) 2370.
[39] E.A. Chandros, A.H. Schiebel, J. Am. Chem. Soc. 95 (1973) 611.
[40] F. Hirayama, J. Chem. Phys. 42 (1962) 3163.
[41] N.J. Leonard, Acc. Chem. Res. 12 (1979) 423.
[42] E. Farkas, M. Hilbert, I. Ketskemety, L. Gati, Spectrochim. Acta 48A (1992) 95.
[43] K. Kasama, K. Kikuchi, Y. Nishida, H. Kokubun, J. Phys. Chem. 85 (1981) 4148.
[44] J. Rak, J. Blazejowski, J. Photochem. Photobiol. A: Chem. 67 (1992) 287.
[45] L.A. Diverdi, M.R. Topp, J. Phys. Chem. 88 (1984) 3447.
[46] J. Rak, J. Blazewjowski, J. Org. Chem. 57 (1992) 3720.
[47] D.G. Whitten, Y.J. Lee, J. Am. Chem. Soc. 93 (1971) 961.
[48] N. Mataga, Y. Kaifu, M. Koizumi, Bull. Chem. Soc. Jpn. 29 (1956) 373.
[49] A. Weller, Z. Elektrochem. 61 (1957) 956.
[50] E.W. Michl, Thulstrup, J. Eggers, Ber. Bunsenges. Phys. Chem. 78 (1974) 575.
[51] D. Fornasiero, T. Kurucsev, Chem. Phys. Lett. 117 (1985) 176.
[52] F. Schael, M.B. Rubin, S. Speiser, manuscript in preparation.
[53] E.S. Pysh, N.C. Yang, J. Am. Chem. Soc. 85 (1963) 2124.
[54] Y.H. Li, L.-M. Chan, L. Tyer, R.T. Moody, C.M. Himel, D.M. Hercules, J. Am. Chem. Soc. 97 (1975) 3118.
[55] K.P. Ghiggino, A.G. Lee, S.T. Meech, D.V. O'Connor, D. Phillips, Biochemistry 20 (1981) 5381.
[56] S.R. Meech, D.V. O'Connor, D. Phillips, J. Chem. Soc., Faraday Trans. 27 (9) (1983) 1563.
[57] S. Suzuki, T. Fujii, J. Mol. Spectrosc. 47 (1973) 243.
[58] H.H. Jaffe, M. Orchin, Theory and Application of Ultraviolet Spectroscopy, Wiley, New York, 1962.
[59] H. Katayama, S. Ito, M. Yamamoto, J. Phys. Chem. 96 (1992) 10115.
[60] J. Chodkowski, A. Chrzanowski, Rosz. Chem. 50 (1976) 935.